Path loss model in typical outdoor environments in the 50-73 GHz band

Sana Salous, X. Raimundo and A.Cheema
School of Engineering and Computing Sciences
Durham University
Durham, UK
Sana.Salous@durham.ac.uk

***Abstract*—Results of path loss in typical outdoor environments in two frequency bands identified in WRC15 for future 5G radio systems are presented. These include angular path loss as estimated from the strongest component, the main beam, the back beam and from the synthesized omni-directional beam.**

Keywords—path loss; polaisation;, 5G; WRC15

I. INTRODUCTION

Wideband channel parameters in the frequency bands above 6 GHz are currently the subject of intense investigation by different research groups including industry and academia. In November 2015, the World Radiocommunications Conference, WRC15 identified a number of frequency bands between 24-86 GHz as possible bands for future 5G wireless communications. To estimate channel parameters such as path loss and delay spread, wideband measurements in typical indoor [1] and outdoor environments were performed which include hilly terrain with roadside vegetation, street canyon, car park and roadside. The measurements were performed at two frequencies in the 50-75 GHz band identified by WRC-15 using the 2 by 2 wideband channel sounder developed at Durham University for multiple input multiple output measurements [2]. To study the impact of polarization, the measurements were performed with dual polarized antennas at the transmitter and at the receiver. The measurements were performed with 6 GHz bandwidth between 51-57 GHz and 67-73 GHz and analysed with 2 GHz bandwidth.

Horn antennas were used at the receiver with a beam width (18.4º in the E plane and 19.7º in the H plane at 50 GHz and 14.4º in the E plane and 15.4º in the H plane at 67.5 GHz). At the transmitter two horn antennas were used and these have beam widths (56.3º in the E plane and 51.4º in the H plane at 50 GHz and 40º in the E plane and 38º in the H plane at 67.5 GHz). To perform dual polarization measurements, a twist was used at one of the transmit channels and another at one of the receive channels. To enable front beam, back beam and the synthesis of non-directional propagation, the receiver was mounted on a turntable which was rotated in 5 degree steps to cover all azimuthal angles.

Following calibration the coefficients of the path loss model for the four polarizations were estimated using the least square fit. The results for the path loss parameters are presented for various beam widths/directions of the receive antenna.

II. MEASUREMENT SCENARIOS AND DATA ANALYSIS

The sounder was used to measure the channel response in different outdoor environments including a road side, a car park, an open square and street canyon as shown in Fig. 1.

Fig. 1. Measured outdoor environments: road side, car park, open square and street canyon

For these measurements, the transmitter and receiver were mounted on trolleys with the transmitter being held in a fixed location with the RF head unit being mounted at about 3 m and the receiver antenna was mounted on the trolley at 1.6 m.

The power delay profile for each angle of arrival was used to estimate the received power above the noise floor. The omni-directional power was estimated by taking the sum of the received power from the power angular profile illustrated in Fig. 2 for one of the locations. The transmitter and receiver used high stability rubidium standards which also enabled the synthesis of the omni-directional power delay profiles as shown in Fig. 3 for the VV and VH polarizations.

Following full calibration of the data, the received power was then used to estimate the path loss for the following antenna beam widths: the maximum received power representing the main beam of the receive antenna; 40^{o} main beam power; the sum of the received power from the remaining angles outside the 40^{o} main beam; and the 360^{o} (omni-directional): the sum from all the azimuthal angles.

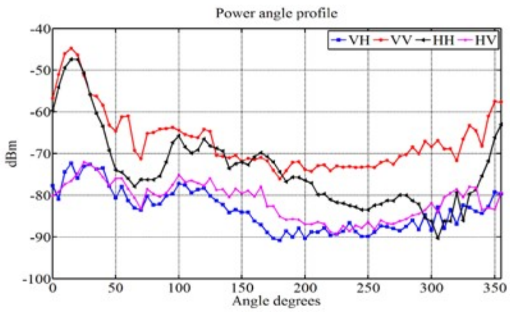

(a)

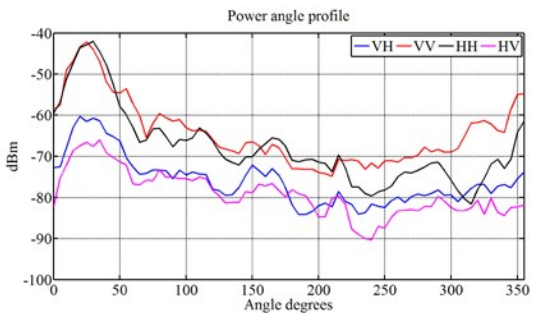

(b)

Fig. 2 Power versus angle of rotation for the dual polarized antennas in the (a) 67-73 GHz, (b) 51-57 GHz

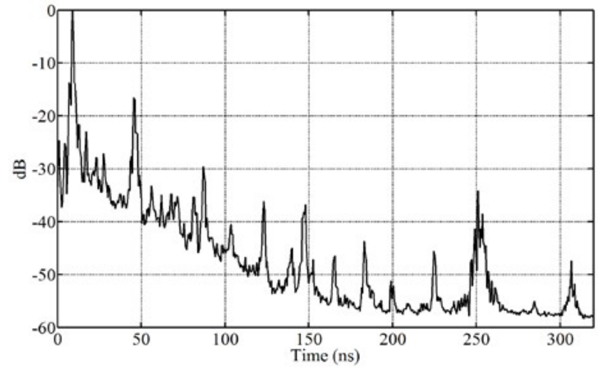

(a)

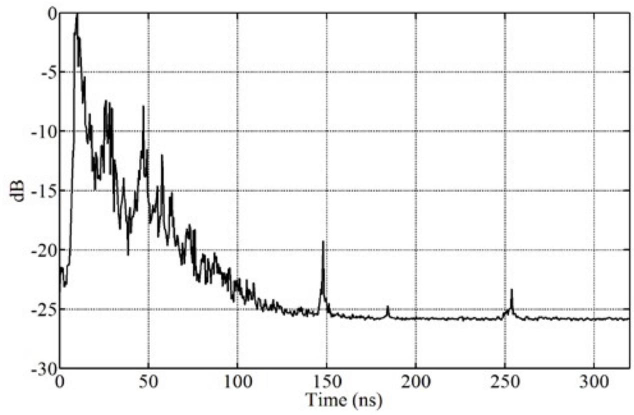

(b)

Fig. 3 Synthesized omni-directional power delay profile (a) VV and (b) VH

In [3] the synthesis of omni-directional path loss from directional measurements is proposed when the rotation angle step is equal to the 3 dB beam width of the antenna. Since the 3 dB beam width of the receive antenna in the present measurements is wider than the angle of rotation, the estimated omnidirectional power has an additional 6 dB gain that needs to be taken into account as illustrated in Fig.4 which displays the measured antenna pattern for co-polarized and cross-polarized antennas and the synthesized omni-directional beam from the sum over all angles of rotation.

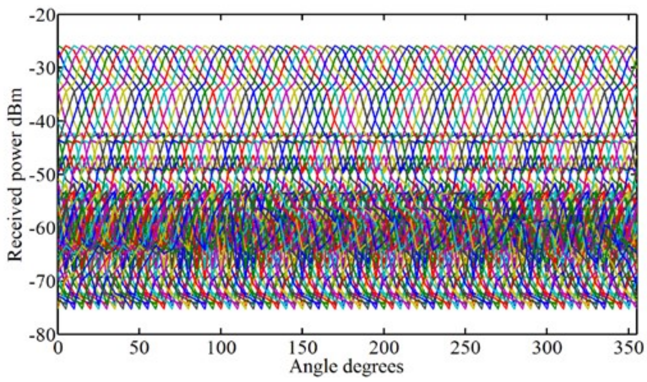

(a)

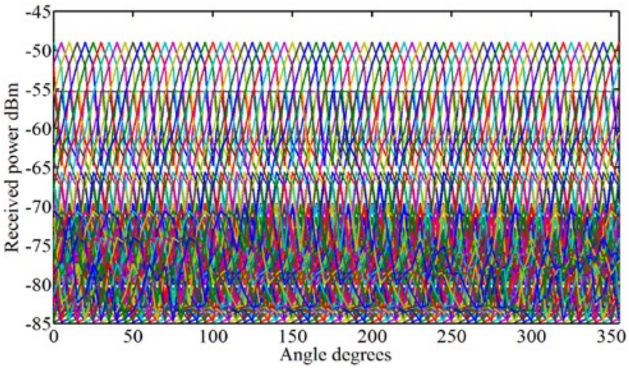

(b)

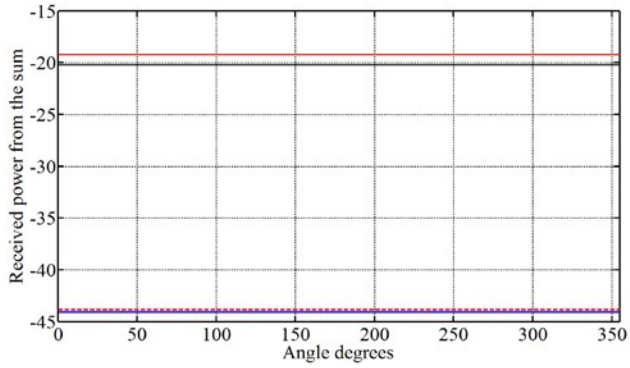

(c)

Fig.4 (a) Super-imposed antenna responses (a) co-polarised (b) cross-polarised, (c) sum of the superimposed responses

III. RESUTS OF PATH LOSS PARAMATERS

The estimated path loss values from each environment for the four polarizations and for the different beam widths were used to estimate the parameters of the path loss model given in equation 1

$$PL(\mathrm{d}) = L_o + 10n\,log10(\mathrm{d}/\mathrm{d}_o) + \mathrm{L}_{gas} + \mathrm{L}_{rain} + \sigma \text{ dB} \quad (1)$$

where n represents the path loss coefficient, L_o is the path loss at a reference distance, d_o, and σ represents the standard deviation of the fit. For frequencies in the higher bands, the additional terms L_{gas} and L_{rain} represent the gaseous absorption and rain attenuation, respectively depending on the frequency and the conditions at the time of measurements. An example of the fit to the measurements is shown in Fig. 5 for the strongest received component for the frequency band 67-73 GHz, with the corresponding path loss parameters in Tables 1 and 2 for the two frequency bands for both the strongest component and the back beam for two of the measured scenarios. The tables indicate an increase in the path loss L_o for the back beam with respect to the front beam as expected and can be observed in Fig. 2. The results for the synthesized omni-directional and the main front beam were fairly close to the strongest component which is expected when the received power is dominated by the Line of Sight (LoS) component. The other scenarios gave a similar trend since all the measurements were performed where the transmitter and receiver were not blocked by buildings with some locations having tree branches along the path.

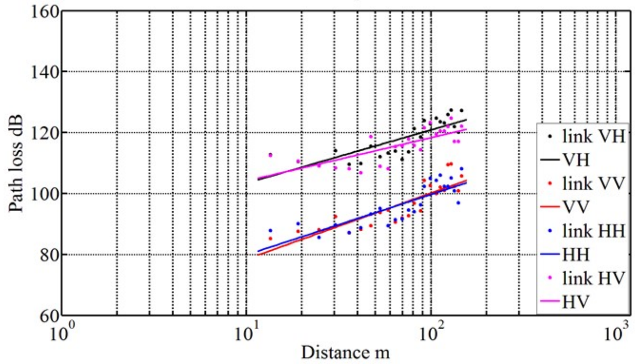

Fig. 5 Path loss fit for the strongest component in the 67-73 GHz frequency band

TABLE 1 Path loss parameters in the street canyon and open square scenario (a) for the strongest component,(b) for the back beam

(a)

Antenna polarization	n, L_o, σ	
	51-57 GHz	67-73 GHz
VH	2.38, 78.12, 2.4	1.74, 97.99, 3.66
VV	2.83, 52.9 , 3.72	2.16, 68.77, 3.76
HH	2.23, 61.82, 3.56	1.98, 71.97, 3.86
HV	2.14, 83.56, 3.05	1.42, 101.87, 3.72

(b)

Antenna polarization	n, L_o, σ	
	51-57 GHz	67-73 GHz
VH	2.31, 78.51, 2.12	2.12, 91.87, 2.92
VV	2.45, 66.01, 2.78	1.72, 84.44, 2.31
HH	1.66, 79.87, 2.09	1.24, 95.50, 2.18
HV	2.26, 86.05, 1.91	2.00, 96.15, 2.10

TABLE 2 Path loss parameters in the car park scenario (a) for the strongest component,(b) for the back beam

(a)

Antenna polarization	n, L_o, σ	
	51-57 GHz	67-73 GHz
VH	2.59, 73.31, 1.89	2.85, 78.99, 2.79
VV	1.93, 67.17, 2.21	2.45, 65.20, 1.92
HH	1.75, 69.56, 1.27	2.51, 65.96, 1.62
HV	2.76, 75.52, 1.63	3.32, 71.60, 2.37

(b)

Antenna polarization	n, L_o, σ	
	51-57 GHz	67-73 GHz
VH	2.07, 81.83, 0.99	2.51, 85.02, 1.67
VV	1.66, 78.13 1.54	2.31, 75.59, 1.60
HH	1.61, 81.87, 1.36	2.07, 84.55, 1.73
HV	2.26, 85.09, 1.52	2.42, 88.13, 2.05

The data from all the measured routes were then combined to generate a single path loss model with the results summarized in Table 3 for the synthesized omni-directional antenna and the back beam.

TABLE 3 Path loss parameters in the car park scenario (a) for the synthesized omni-directional beam,(b) for the back beam

(a)

Antenna polarization	n, L_o, σ	
	51-57 GHz	67-73 GHz
VH	2.6, 54.9, 4.8	2.3, 64.9, 3.9
VV	2.4, 58.7, 4.7	2.2, 69.0, 4.3
HH	2.1, 78.5, 3.0	2.1, 88.5, 3.6
HV	2.1, 82.7, 3.2	2.2, 86.5, 3.9

(b)

Antenna polarization	n, L_o, σ	
	51-57 GHz	67-73 GHz
VH	2.5, 65.3, 4.6	2.2, 76.7, 3.5
VV	2.1, 74.2, 5.0	1.8, 88.5, 4.1
HH	3.0, 67.2, 5.0	2.4, 86.4, 4.29
HV	2.5, 82.8, 8.5	2.5, 87.4, 3.49

IV. CONCLUSIONS

Measurements in various outdoor environments representative of below the roof top were performed on the campus of Durham University. The data were analyzed to estimate the path loss model for two of the WRC15 identified frequency bands in the 50-75 GHz V band. Both the omni-directional path loss and the back beam path loss parameters were estimated. Since the measurements were performed in un-obstructed environment, the omni-directional, the front beam and the strongest component path loss parameters were very close with the back beam path loss being higher. Thus for the un-obstructed scenario, it is sufficient to measure the strongest component and the back beam received power which is representative of the user's movement away from the direction of the transmitter. Taking the vertical to vertical polarization for the 51-57 GHz band, the path loss parameters n and L_o, are 2.4, 58.7 for the omni-directional antenna in comparison to 2.1, 74.2 which highlights the additional path loss experienced when the user moves away from the direction of the transmitter. Further measurements using omni-directional antennas in both line of sight scenarios and non-line of sight scenarios are planned to derive a suitable path loss model for the higher frequency bands. The path loss models presented in this paper are for each frequency separately. For future work, it is desirable to obtain a path loss model across a number of frequency bands. This would be particularly relevant for line of sight scenarios. The effect of beam width on the mm wave channel characteristics was also investigated in [4] and further work on the impact of beam width on delay spread is underway.

ACKNOWLEDGMENT

The 60 GHz sounder was developed under the EPSRC grant PATRICIAN EP/I00923X/1. The upgrade to the WRC15 frequency bands and the measurements reported in the paper are funded under an Ofcom contract Number 1362 on 'Long term measurements campaign and development of model(s) for mm wave bands (30-90 GHz)'.

REFERENCES

[1] S. Salous, S. M. Feeney, X. Raimundo and A. A. Cheema, "Wideband MIMO Channel Sounder for Radio Measurements in the 60 GHz Band," in IEEE Transactions on Wireless Communications, vol. 15, no. 4, pp. 2825-2832, 2016.

[2] X. Raimundo, S. Salous, and A. A. Cheema, Indoor radio propagation measurements in the V-band, to be presented at the IET Workshop on Radio Propagation and Technologies for 5G, 3rd October 2016, Durham, UK

[3] S. Sun, G. MacCartney, M. Samimi, and T. Rappaport,"Synthesizing Omnidirectional Antenna Patterns, Received Power and Path Loss from Directional Antennas for 5G Millimeter-Wave Communications," 2015 IEEE Global Communications Conference (Globecom), 2015.

[4] M.Kim, J. Liang, J. Lee, J. Park, B. Park, and H.Kyu Chung
[Invited] Investigating the Effect of Antenna Beamwidth on Millimeter-wave Channel Charaterization
Myung-Don Kim, Jinyi Liang, Juyul Lee, Jaejoon Park, Bonghyuk Park and Hyun Kyu Chung
Electronics and Telecommunications Research Institute, Korea